Bioorganic Chemistry 93 (2019) 103319

Contents lists available at ScienceDirect

Bioorganic Chemistry

journal homepage: www.elsevier.com/locate/bioorg

Design, synthesis and biological evaluation of resveratrol-cinnamoyl derivates as tubulin polymerization inhibitors targeting the colchicine binding site

Yong Yin, Bao-Ping Lian, Yuan-Zheng Xia, Yu-Ying Shao, Ling-Yi Kong*

Jiangsu Key Laboratory of Bioactive Natural Product Research and State Key Laboratory of Natural Medicines, Department of Natural Medicinal Chemistry, School of Traditional Chinese Pharmacy, China Pharmaceutical University, 24 Tong Jia Xiang, Nanjing 210009, People's Republic of China

ARTICLE INFO

Keywords:
Resveratrol-cinnamoyl derivates
Tubulin polymerization inhibitors
Colchicine binding site
Anti-proliferative

ABSTRACT

A novel series of resveratrol-cinnamoyl hybrids as tubulin polymerization inhibitors were designed and synthesized, and evaluated for their anti-proliferative activities against A549, MCF-7, HepG2, HeLa and MDA-MB-231 five cancer cell lines. Most designed compounds showed better anti-proliferative activities. Particularly, compound **6h** exhibited the potent anti-proliferative activities with the IC_{50} value of 0.12, 0.016, 0.44, 0.37 and 0.78 μM against A549, MCF-7, HepG2, HeLa and MDA-231, respectively, which was superior to that of reference drug colchicine. Besides, compound **6h** displayed a remarkable inhibition of tubulin polymerization and a great potency to compete with [^{3}H] colchicine in binding to tubulin. Further studies indicated that compound **6h** could induce the MCF-7 cells arrest in the G2/M phase. What' more, compound **6h** induced cell apoptosis in a dose-dependent manner, and regulated the expression level of apoptosis-related proteins. These results revealed that compound **6h** is a promising tubulin polymerization inhibitor for treatment of cancer and it is worthy of further exploitation.

1. Introduction

It has been recognized that microtubules play a critical role in regulating many cellular processes such as cellular proliferation and division, motility and shape maintenance, spindle formation, intracellular transportation and so on [1–4]. Microtubules are cylindrical structures and crucial components of cytoskeleton which made of α- and β-tubulin heterodimers in eukaryotic cells, and the heterodimers are always a highly dynamic equilibrium processes of polymerization and depolymerization, it is identified to be a critical characteristic of microtubule [5–8]. Breaking the dynamic equilibrium lead to disrupt the cell division, resulting in an increase in a large number of cells in metaphase arrest, and then cell death [9–11]. So tubulin has been well known to be an attractive target for exploring new anticancer agents [12].

Over the past decades, a large number of tubulin inhibitor have been developed and identified, and they are classified into two categories, one class is microtubule destabilizing agents which binding to the colchicine and vinblastine binding site and interfering with tubulin assembly, the other class is microtubule-stabilizing agents which binding to the tubulin paclitaxel binding site and disturbing the tubulin disassembly [13–16]. However, there is no candidate molecule binding at the colchicine site can be approved by FDA in the decades.

Nowadays, many tubulin inhibitors binding at the colchicine site have been designed and explored, such as Colchicine, CA-4, SAMRT and so on (Fig. 1) [5,17,18]. Many 4,5-dihydro-1*H*-pyrazole derivates (**1**) were developed to inhibit tubulin assembly, as can been see, the flexible of these tubulin inhibitors was enhanced and they can well bind the colchicine site, resulting in the potent anticancer activity [19–21]. Besides, chalcone derivates show the potent anticancer activity as tubulin inhibitor [22], and the framework was also employed to modify some natural compound as tubulin inhibitor, such as resveratrol, which showed the potent antiproliferative and proapoptotic effects on human cancer cells [23,24]. Chalcone-resveratrol derivates were explored to be tubulin inhibitor but the more rigidity of the compound was improved, it may lead to some unwanted side effect which limit the further preclinical study [22].

In order to improve the flexible of compound, the acyl ester group was introduced, which make compound bind well to the target protein. Meanwhile, the key fragments were remained, such as the α,β-unsaturated ketone of chalcone and methoxy group. Based on these strategies, a novel series of resveratrol-cinnamoyl derivates as tubulin

* Corresponding author.
E-mail address: cpu_lykong@126.com (L.-Y. Kong).

https://doi.org/10.1016/j.bioorg.2019.103319
Received 25 May 2019; Received in revised form 16 September 2019; Accepted 26 September 2019
Available online 26 September 2019
0045-2068/

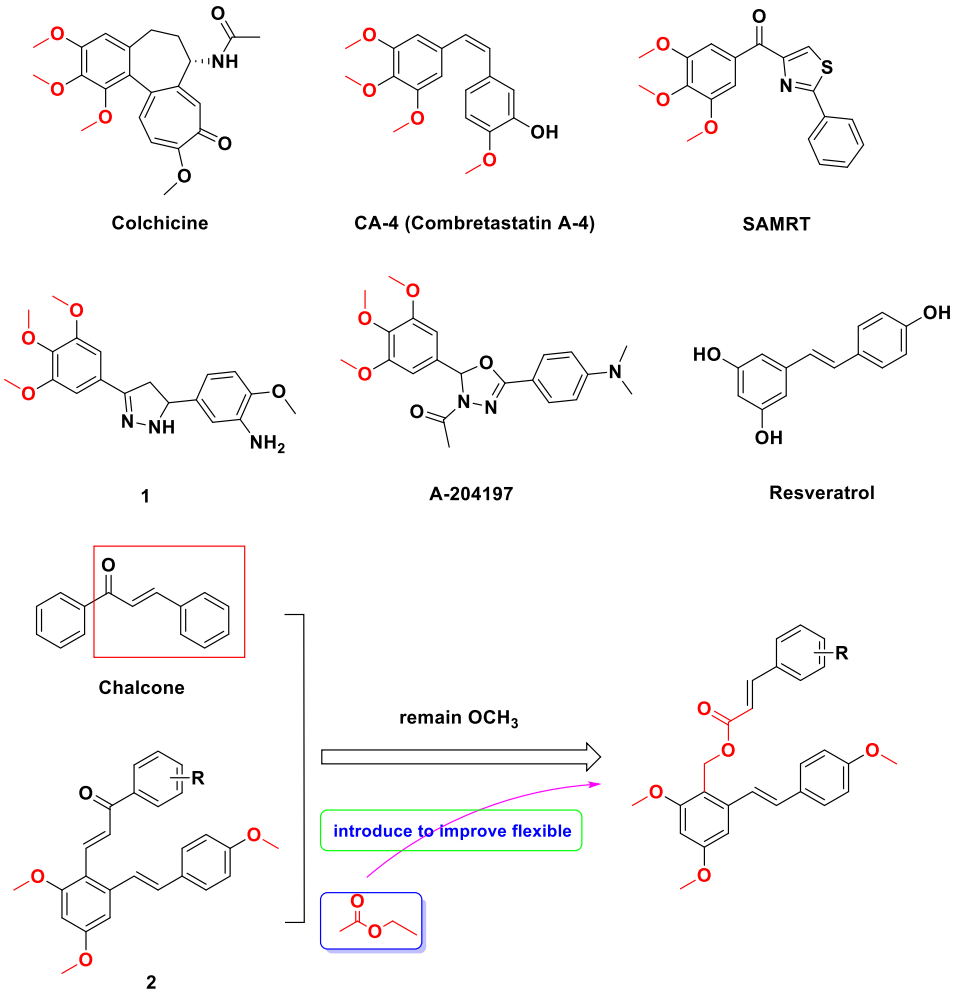

Fig. 1. The structure of tubulin assembly inhibitors and the strategy of molecular design.

inhibitors were designed, and the bioactivities of these compounds was evaluated. Molecular docking was also performed to explore the binding modes of these compounds at the colchicine binding site.

2. Results and discussion

2.1. Chemistry

The desired compounds were synthesized as described in the Scheme 1. Methylation of resveratrol and then get the compound **3** using Vilsmeier-Haack reaction ($POCl_3$/DMF). Compound **3** was reduced under $NaBH_4$ catalyzing to obtain compound **4**. Subsequently, compound **4** and various cinnamic acid were reacted to get the targeted compounds (**6a–6o**).

2.2. Anti-proliferative activities in vitro

All the desired compounds were evaluated the anti-proliferative activities against A549, MCF-7, HepG2, HeLa and MDA-MB-231 five cancer cell lines using the 3-(4,5-dimethyl-2-thiazolyl)-2,5-diphenyl-2-H-tetrazolium bromide (MTT) assay. Meanwhile, as colchicine site tubulin inhibitor, colchicine and CA-4 were selected to be positive drug. The results were summarized in Table 1. As can be seen, most compounds exhibited good anti-proliferative activities against the five cancer cell lines, and the IC_{50} value of five compounds (**6f**, **6h**-**6k**) were no more than 5 μM. Meanwhile, all the designed compounds showed low toxicity against human normal hepatocytes LO2 cells (the CC_{50} value ranged from 87.37 to 167.44 μM) and human embryonic kidney 293T cells (the CC_{50} value ranged from 93.61 to 127.79 μM). Particularly, compound **6 h** displayed the potent anti-proliferative activity with the IC_{50} value of 0.12, 0.016, 0.44, 0.37 and 0.78 μM against A549, MCF-7, HepG2, HeLa and MDA-231, respectively. It was superior to that of the reference drug colchicine, and not much worse than CA-4.

It was interesting to find that compound **6h** containing methoxy group showed the potent activities, indicating that the methoxy group play an important role in improvement of anti-proliferative activity, and some compounds containing the group such as **6d**-**6f** also displayed a certain extent of anti-proliferative activity. Meanwhile, when the methoxy substituted in *ortho*-position, the compound exhibited the unfavorable activity against the five cancer cell lines, such as compound **6c** and **6g**. What's more, the substituent in the benzene ring of cinnamoyl affected the activities of compounds, compound with the halogen substituent also exhibited the better anti-proliferative activity, and the tendency of the order is F > Br > Cl. Besides, compounds (**6n**, **6o**) containing electron with-drawing groups (NO_2, CF_3) displayed the poor anti-proliferative activity, and the electron with-drawing groups (NO_2, CF_3) have no contribute to the anti-proliferative activity of compounds. In summarized, electron-donating group (such as OCH_3) in the benzene ring of cinnamoyl could helpful to improve the anti-proliferative activity. In contrast, the electron with-drawing groups (NO_2, CF_3) in the benzene ring could decrease activities of compounds.

Meanwhile, compound **6h** was selected to evaluate the anti-proliferative activity against some drug resistant cancer cells to investigate its effect on drug resistant cancer cells. The result was shown in Table 2,

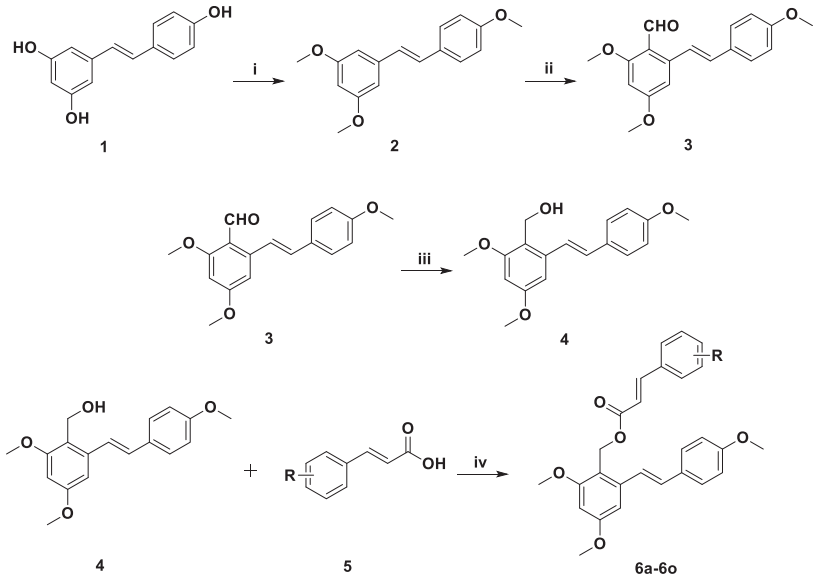

compound	R	compound	R
6a	H	**6i**	4-F
6b	4-CH_3	**6j**	3-Cl
6c	2-OCH_3	**6k**	4-Cl
6d	3-OCH_3	**6l**	3-Br
6e	4-OCH_3	**6m**	4-Br
6f	3,4-OCH_2O-	**6n**	4-NO_2
6g	2,3,4-OCH_3	**6o**	4-CF_3
6h	3,4,5-OCH_3		

Scheme 1. Synthesis of the desired compounds **6a-6o**. Reagents and conditions: (i) CH_3I/K_2CO_3, acetone, reflux; (ii) $POCl_3$/DMF, 0°C-rt.; (iii) $NaBH_4$, EtOH, rt; (iv) DCC/DMAP, DCM, reflux.

compound **6h** exhibited the 14-fold resistances to the corresponding drug-resistant cells, which was similar to CA-4. Compared to taxol and vincristine, compound **6h** revealed the moderate antiproliferative activity against drug resistant cancer cells.

2.3. Tubulin polymerization inhibitory in vitro

To evaluate whether these resveratrol-cinnamoyl derivates target the tubulin-microtubule system, the representative compounds (**6f**, **6h**-**6m**) were selected to test their inhibitory activities against tubulin polymerization in vitro. As can be seen in Table 3, compound **6h** exhibited the potent activity in inhibiting tubulin polymerization and the IC_{50} value was 1.03 μM, slightly better than that of the reference compound CA-4 (IC_{50} = 1.32 μM). As shown in Fig. 2, colchicine exhibited a significant inhibition of tubulin polymerization. Interestingly, compound **6h** displayed the superior action to that of colchicine, it was indicated that compound **6h** could be an anti-tubulin inhibitor. Meanwhile, compound **6h** was also tested for potential inhibition of the binding of [^{3}H] colchicine to tubulin and the result was listed in Table 3, indicating that compound **6h** competed with [^{3}H] colchicine in binding to tubulin, the binding potency to the colchicine binding site was up to 91.31% at 4 μM, identifying that compound **6h** display the tubulin polymerization inhibition and bind to the colchicine binding site.

2.4. Induce cell cycle arrest

Most tubulin destabilizing agents generally could disrupt the mitosis to arrest normal cell cycle, lead to decrease growth and proliferation of cancer cells. The effect of **6h** on MCF-7 cell cycle progression was examined by flow cytometry analysis using PI staining assay. The results were showed in Fig. 3, compound **6h** could induce the MCF-7 cell arrest in the G2/M phase, which increased to 77% at 1 μM. What's more, the percentage of cells at the G2/M phase from 13.92 to 77%, indicating compound **6h** induced a markedly cell cycle arrest at the G2/M phase in a dose-dependent manner, compared to 12.92% of untreated control.

Moreover, the alterations in G2/M regulatory protein expressions were studied after treatment of compound **6h** in MCF-7 cell. As shown in Fig. 3, compound **6h** caused a decrease in CDK1 expression and CDC25C expression, resulting cell cycle arrest in G2/M phase, and the expression of p-CDK1 was up-regulated. All the results exhibited the dose-dependent manner.

Table 1
The antiproliferative activities of all designed compounds against cancer cell lines.

Compounds	IC_{50} ± SD (μM)[a]					CC_{50} ± SD (μM)[b]	
	A549	MCF-7	HepG2	HeLa	MDA-MB-231	LO2	293 T
6a	7.19 ± 0.25	4.32 ± 0.37	8.48 ± 0.63	9.10 ± 1.03	12.13 ± 1.47	112.43 ± 9.14	97.68 ± 8.83
6b	28.96 ± 1.08	23.65 ± 2.03	19.17 ± 1.81	27.83 ± 2.58	29.52 ± 3.04	108.56 ± 9.66	102.17 ± 9.18
6c	> 50	46.82 ± 2.41	49.91 ± 3.79	> 50	> 50	–	–
6d	12.47 ± 0.94	8.37 ± 0.94	11.78 ± 1.42	11.49 ± 1.42	18.62 ± 2.06	143.82 ± 8.41	112.73 ± 8.64
6e	17.83 ± 0.88	14.19 ± 0.98	21.03 ± 1.65	19.46 ± 2.35	32.87 ± 2.89	167.44 ± 10.62	94.88 ± 9.05
6f	0.87 ± 0.01	0.091 ± 0.003	0.51 ± 0.03	0.49 ± 0.038	2.86 ± 0.19	98.13 ± 10.13	113.26 ± 9.63
6g	49.86 ± 1.79	> 50	> 50	47.16 ± 3.18	> 50	–	–
6h	0.12 ± 0.008	0.016 ± 0.001	0.44 ± 0.004	0.37 ± 0.012	0.78 ± 0.03	126.48 ± 11.45	103.47 ± 7.19
6i	0.98 ± 0.01	0.23 ± 0.02	0.76 ± 0.02	1.17 ± 0.11	1.94 ± 0.17	103.65 ± 9.86	93.61 ± 7.84
6j	1.39 ± 0.02	0.88 ± 0.03	1.19 ± 0.07	1.92 ± 0.14	3.04 ± 0.28	112.78 ± 8.47	107.75 ± 8.26
6k	1.46 ± 0.02	1.03 ± 0.11	1.21 ± 0.09	2.84 ± 0.21	3.76 ± 0.21	87.37 ± 6.83	102.43 ± 6.59
6l	3.95 ± 0.18	2.17 ± 0.23	5.18 ± 1.44	7.46 ± 0.44	9.13 ± 0.76	94.18 ± 7.37	127.79 ± 9.17
6m	2.07 ± 0.23	2.29 ± 0.18	3.04 ± 1.76	4.68 ± 0.67	5.77 ± 0.68	104.31 ± 9.14	101.82 ± 10.13
6n	48.74 ± 2.44	> 50	38.81 ± 4.82	44.37 ± 3.78	> 50	–	–
6o	> 50	> 50	44.75 ± 4.13	> 50	47.43 ± 3.78	–	–
Colchicine[c]	1.17 ± 0.013	0.74 ± 0.002	1.33 ± 0.07	1.08 ± 0.05	3.01 ± 0.22	9.16 ± 0.62	8.34 ± 0.71
CA-4[c]	0.15 ± 0.006	0.037 ± 0.005	0.18 ± 0.009	0.014 ± 0.003	0.056 ± 0.008	0.28 ± 0.004	1.07 ± 0.013

[a] IC_{50} values are indicated as the mean ± SD (standard error) of at least three independent experiments.
[b] Cytotoxicity in human normal cell.
[c] Used as positive control.

2.5. Induce cell apoptosis

To identify if the compound **6h** could induce cell apoptosis in MCF-7 cell, apoptosis assay was explored using Annexin V-FITC/PI assay. As shown in Fig. 4, after treatment by compound **6h** for 48 h at different concentrations (0.25, 0.5, and 1 μM), the percentage of late apoptotic cells from 7.5 to 33.0%, and the percentage of early apoptotic cells from 0.3 to 11.1%, indicating that compound **6h** is very effective in the induction of apoptosis in a dose-dependent manner.

Besides, apoptosis-related proteins were examined in MCF-7 cells after treatment by compound **6h**, and the results were also showed in Fig. 4. As can be seen, the level expression of proapoptotic protein Bax was increased by **6h** treatment in a dose-dependent manner. In contrast, the anti-apoptotic protein Bcl-2 expression was decreased. In addition, the expression level of Cleaved-PARP and Cleaved Caspase-3, which were the marker of cells undergoing apoptosis, were both up-regulated by treatment with **6h** in a dose-dependent manner. All the results conform to cell apoptosis results.

2.6. Immunofluorescence of compound *6h*

In order to investigate the effects of compound 6h to microtubules in living cells, immunofluorescence assay in MCF-7 cells by staining tubulin was carried out. As shown in Fig. 5, cells in the control group exhibited the normal arrangement and organization, the microtubule network was well-assembled. In contrast, after treatments with colchicine (0.25 μM) and **6h** at different concentrations (0.25, 0.5 μM) for 24 h, respectively, cell morphology has been changed and the cytoskeleton was destroyed, the microtubule networks were broken down. It was indicated that compound **6h** could disturb the assemble of microtubule and be a novel tubulin polymerization inhibitor.

Table 3
Inhibition of tubulin polymerization and colchicine binding to tubulin.

Compounds	Inhibition of tubulin polymerization IC_{50} ± SD (μM)[a]	Inhibition of colchicine binding (% inhibition ± SD)[b]	
		2 μM	4 μM
6f	3.72 ± 0.11	–	–
6h	1.03 ± 0.09	81.74 ± 1.72	91.31 ± 1.66
6i	3.48 ± 0.13	–	–
6j	4.47 ± 0.43	–	–
6k	4.63 ± 0.28	–	–
6l	8.29 ± 0.57	–	–
6m	6.44 ± 0.44	–	–
CA-4	1.32 ± 0.11	82.23 ± 1.47	91.46 ± 1.58

[a] Data are presented as mean from three independent experiments.
[b] Tubulin, 1 μM; [^{3}H]-colchicine, 4 μM; and inhibitors, 2 or 4 μM.

2.7. Molecular modelling

In order to better understand the mode of compound **6h** binding to tubulin, molecular docking of **6h** into the colchicine binding pocket of tubulin (PDB: 1SA0) was performed using Discovery Studio 3.5 software. As shown in Fig. 6A and B, compound **6h** could well bind to colchicine site of tubulin, and the binding mode was similar to that of colchicine. 3,4,5-Trimethoxyphenyl of **6h** was formed a hydrogen bond (distance: 2.02 Å) with Cys241, which is a critical amino acid that

Table 2
The IC_{50} values of compound **6h** in different drug-resistant cancer cells.

Compounds	IC50 ± SD (μM)								
	A549	A549/Taxol	DRI[a]	HCT-8	HCT-8/Taxol	DRI[a]	K562	K562/Vincristine	DRI[a]
6h	0.12 ± 0.008	1.62 ± 0.011	13.5	0.18 ± 0.009	2.24 ± 0.012	12.4	0.094 ± 0.004	1.32 ± 0.012	14.0
CA-4	0.15 ± 0.006	1.47 ± 0.013	9.8	0.034 ± 0.004	0.19 ± 0.012	5.6	0.018 ± 0.009	0.13 ± 0.006	7.2
Taxol	0.027 ± 0.006	2.01 ± 0.037	74.4	0.023 ± 0.004	2.66 ± 0.12	115.7	ND[b]	ND[b]	
Vincristine	ND[b]	ND[b]		ND[b]	ND[b]		0.02 ± 0.005	5.38 ± 0.37	192.1

[a] DRI: drug-resistant index = (IC_{50} of drug resistant cancer cell)/(IC_{50} of parental cancer cell).
[b] ND: not detected.

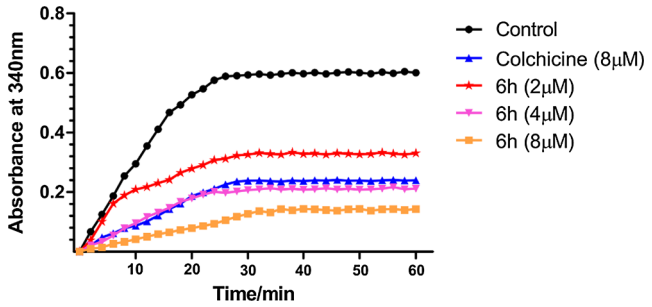

Fig. 2. Effects of **6h** on tubulin polymerization in vitro. Polymerizations were followed by an increase in fluorescence emission at 340 nm over a 60 min period at 37 °C. The experiments were performed three times.

anchors most of all CBS inhibitors [25], and the same interaction was found in the mode of colchicine binding to tubulin, the distance was 1.91 Å. In contrast, the π-cation interaction (formed by benzene ring and Lys352) formed **6h** and tubulin instead of the hydrogen bond (distance: 2.29 Å) (formed by carbonyl and Val181) formed colchicine and tubulin. In the 3D model, it was observed that flexible of compound was improved by introducing the acyl ester group, resulting in **6h** binding to the colchicine site of tubulin with the great conformation. It was proved that the original strategy which introducing the acyl ester group to improve the flexible of desired compound is rational.

3. Conclusion

In summary, a novel series of resveratrol-cinnamoyl derivates as tubulin inhibitors were designed and synthesized, and their anti-proliferative activities against A549, MCF-7, HepG2, HeLa and MDA-MB-231 five cancer cell lines were evaluated, and most desired compounds showed better anti-proliferative activity. Out of them, compound **6h** exhibited the potent anti-proliferative activity (IC_{50} ranging from 0.016 to 0.78 μM), which was superior to that of reference drug colchicine. In addition, compound **6h** exhibited a significant inhibition of tubulin polymerization and a great potency to compete with [^{3}H] colchicine in binding to tubulin. Further pharmacological studies indicated that compound **6h** disturb the dynamic equilibrium processes of microtubule, inhibit tubulin polymerization, lead to cells cycle arrest in G2/M phase, make the cell cycle associated protein CDK1 and CDC25C down-regulate, p-CDK1 up-regulate. Meanwhile, compound **6h** induced cell apoptosis in a dose-dependent manner, the apoptosis-related proteins such as Bax, Cleaved-PARP and Cleaved Caspase-3 were increased, Bcl-2 was decreased. Molecular docking demonstrated that **6h** bind to the colchicine binding site of tubulin. In a word, these results revealed that compound **6h** is a novel tubulin polymerization inhibitor for treatment of cancers, and it deserve to be explored furtherly.

4. Experimental

4.1. Chemistry

All the chemical agents were purchased from commercial suppliers and used without further purification. Reaction progress was monitored by analytical thin layer chromatography (TLC), which was performed on precoated silica gel GF254 plates (Qingdao Haiyang Chemical Plant, Qingdao, China) and the spots were detected by UV light (254 nm). ^{1}H NMR and ^{13}C NMR spectra were measured on a Bruker 500 and 600 spectrometer. Chemical shifts (d) are in parts per million (ppm) downfield from TMS (d); multiplicity; observed coupling constant (J) in hertz (Hz); proton count; assignment. Multiplicities are recorded as s (singlet), d (doublet), dd (doublet of doublet), t (triplet), q (quarter), m (multiplet) and br s (broad singlet) where appropriate. Mass spectra were obtained on a MS Agilent 1100 Series LC/MSD Trap mass spectrometer (ESI-MS).

4.1.1. Synthesis of intermediate 4

Intermediate **4** was synthesized as described in the literature [26,27].

To a solution of resveratrol (**1**) (1 mmol) in 30 ml acetone, potassium carbonate (6 mmol) was added after iodomethane (6 mmol) added. After stirring for 6 h at refluxing temperature, the mixture was cooled down and then filtered, and the solvent was removed to obtain

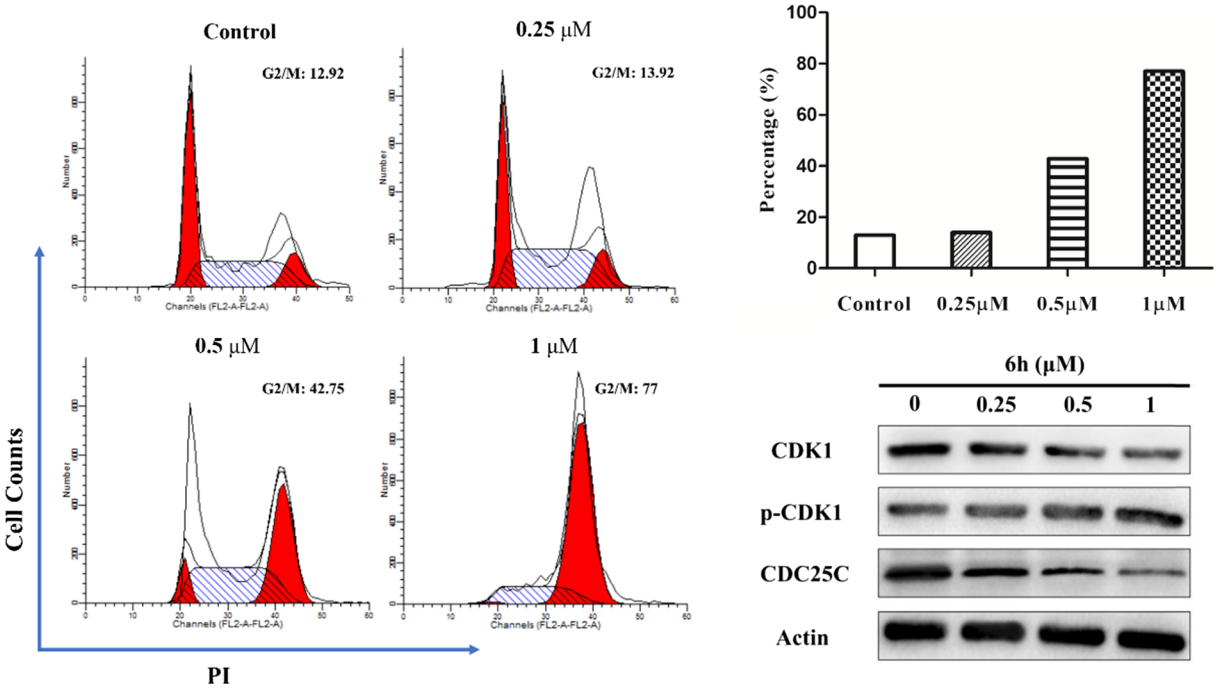

Fig. 3. Compound **6h** induced G2/M arrest in MCF-7 cells. MCF-7 cells were incubated with varying concentrations of **6h** (0, 0.25, 0.5, and 1 μM) for 48 h. Cells were harvested and stained with PI and then analyzed by flow cytometry.

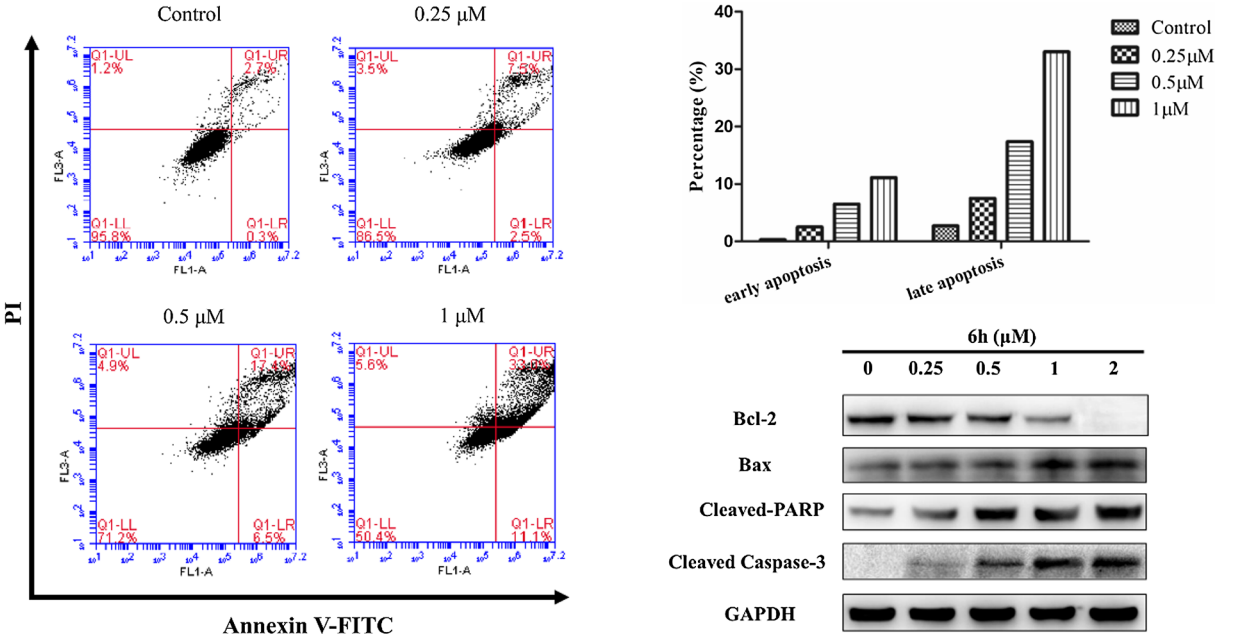

Fig. 4. Compound **6h** induced apoptosis in MCF-7 cells. Cells were collected and stained with Annexin V/PI followed by flow cytometric analysis. MCF-7 cells were incubated with varying concentrations of **6h** (0, 0.25, 0.5, and 1 μM). After 48 h of incubation, cells were collected and stained with Annexin V/PI, followed by flow cytometric analysis.

the crude products, which were purified by column chromatography with EtOAc/PE (1:3) to afford the intermediate **2**.

To a solution of intermediate **2** (1 mmol) in 15 ml anhydrous DMF, phosphorus oxychloride (1.5 mmol) was added dropwise at 0 °C or in the ice-bath. After vigorous stirring for 3 h in the ice-bath, the mixture was poured into 100 ml ice water and stirred for 30 min. The crude product was precipitated and filtered, purified by recrystallization from ethanol to get the intermediate **3**. ^{1}H NMR (DMSO-d_6, 500 MHz): 10.41 (s, 1H, CHO), 7.95 (d, J = 16.25 Hz, 1H, ArH), 7.50 (d, J = 8.70 Hz, 2H, ArH), 7.20 (d, J = 16.25 Hz, 1H, ArH), 6.97 (d, J = 8.70 Hz, 2H, ArH), 6.90 (d, J = 1.90 Hz, 1H, ArH), 6.62 (d, J = 2.10 Hz, 1H, ArH), 3.92 (s, 3H, OCH_3), 3.90 (s, 3H, OCH_3), 3.78 (s, 3H, OCH_3).

Intermediate **3** (1 mmol) was dissolved in 15 ml anhydrous ethanol, sodium borohydride (1 mmol) was added in the ice-bath. After stirring for 2 h at room temperature, the solvent was removed to afford the crude product (intermediate **4**), and it was used to next reaction without further purification.

*4.1.2. The general procedure for the preparations of compounds **6a-6o***

To a solution of intermediate **4** (1 mmol) and various cinnamic acid (1 mmol) in 20 ml anhydrous DCM, dicyclohexylcarbodiimide (1.2 mmol) and 4-dimethylaminopyridine (1 mmol) were added. After stirring for 10 h at refluxing temperature, the mixture was washed by water (2 × 10 ml), and then washed with brine, dried over anhydrous

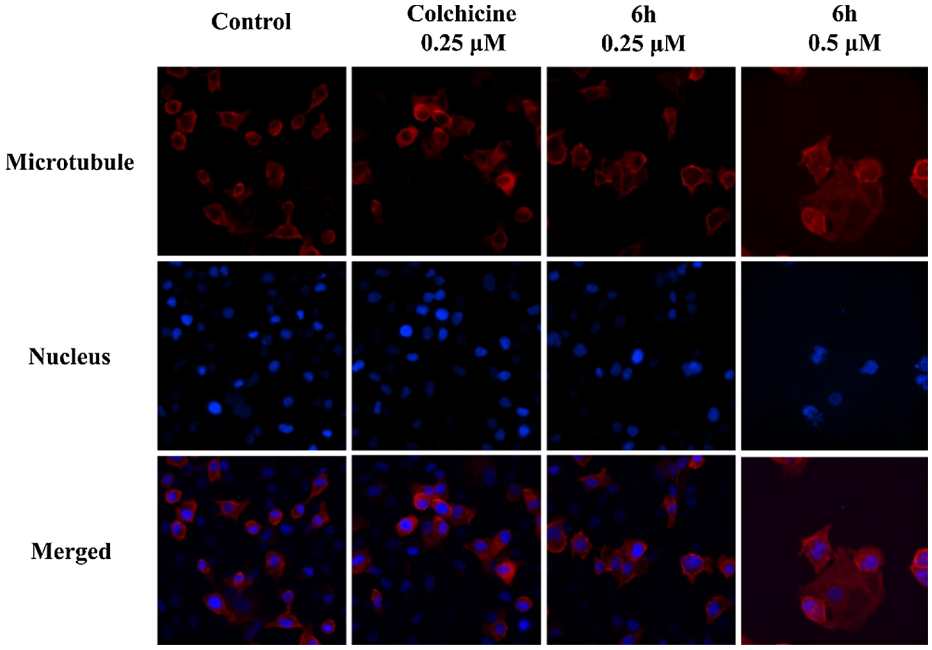

Fig. 5. Effects of **6h** on the cellular microtubule networks visualized by immunofluorescence in MCF-7 cells. Tubulins labeled with Cy3 (red) and nuclei tagged with DAPI (blue) were observed with a confocal fluorescence microscope. MCF-7 cells were treated with vehicle control 0.1% DMSO, Colchicine (0.25 μM), **6h** (0.25 μM), and **6h** (0.5 μM). (For interpretation of the references to colour in this figure legend, the reader is referred to the web version of this article.)

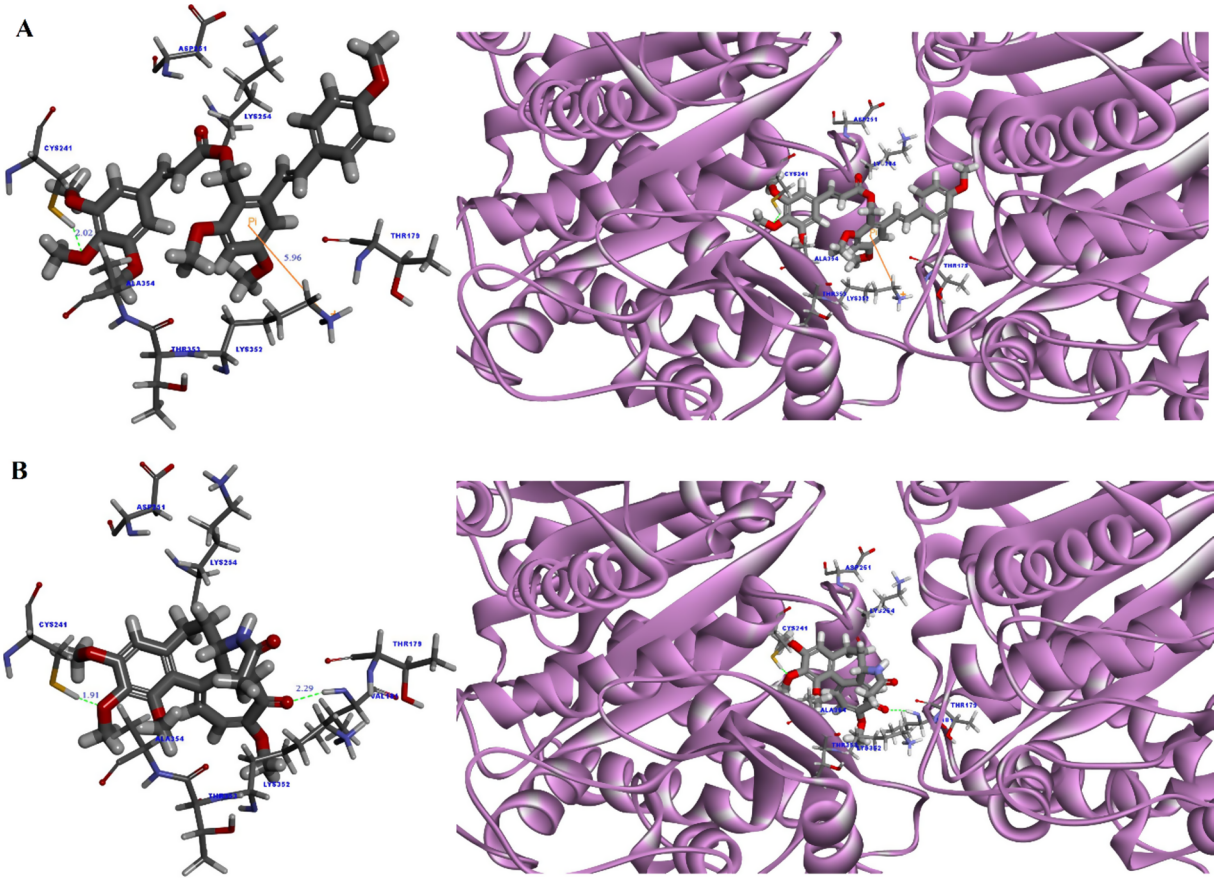

Fig. 6. (A) Molecular docking of **6h** with tubulin (PDB ID: 1SA0). (B) Molecular docking of colchicine with tubulin.

sodium sulfate, and removed in vacuo to get the crude product, which was purified by column chromatography with EtOAc/PE (1:5) to obtain the desired compounds **6a-6o**.

*4.1.2.1. 2,4-Dimethoxy-6-((E)-4-methoxystyryl)benzyl cinnamate (**6a**).* White powder. Yield: 73.7%. m. p: 206–208 °C. ^{1}H NMR (500 MHz, $CDCl_3$): 7.68(d, J = 16.00 Hz, 1H, ArH), 7.45(m, 4H, ArH), 7.33(m, 3H, ArH), 7.31(d, J = 16.05 Hz, 1H, ArH), 6.98(d, J = 16.05 Hz, 1H, ArH), 6.88(d, J = 8.70 Hz, 2H, ArH), 6.78(d, J = 2.25 Hz, 1H, ArH), 6.46(d, J = 16.30 Hz, 1H, ArH), 6.43(d, J = 3.10 Hz, 1H, ArH), 5.44(s, 2H, CH_2), 3.88(s, 3H, OCH_3), 3.85(s, 3H, OCH_3), 3.81(s, 3H, OCH_3). ^{13}C NMR (150 MHz, $CDCl_3$): 167.31, 161.03, 159.89, 159.56, 144.71, 140.62, 134.06, 131.50, 130.16(2), 129.94, 128.83(2), 128.08(2), 123.50, 118.33, 117.25, 114.19(2), 101.83, 97.68, 57.85, 55.90, 55.44, 55.34. MS (ESI) *m/z*: 431.22 $[M + H]^+$ (calcd for 431.18, $C_{27}H_{27}O_5$).

*4.1.2.2. 2,4-Dimethoxy-6-((E)-4-methoxystyryl)benzyl(E)-3-(p-tolyl) acrylate (**6b**).* White powder. Yield: 83.4%. m. p: 216–218 °C. ^{1}H NMR (500 MHz, $CDCl_3$): 7.66(d, J = 15.95 Hz, 1H, ArH), 7.45(d, J = 8.70 Hz, 2H, ArH), 7.36(d, J = 8.10 Hz, 2H, ArH), 7.31(d, J = 16.05 Hz, 1H, ArH), 7.15(d, J = 7.95 Hz, 2H, ArH), 6.99(d, J = 16.05 Hz, 1H, ArH), 6.88(d, J = 8.75 Hz, 2H, ArH), 6.79(d, J = 2.30 Hz, 1H, ArH), 6.44(d, J = 2.30 Hz, 1H, ArH), 6.41(J = 15.95 Hz, 1H, ArH), 5.44(s, 2H, CH_2), 3.88(s, 3H, OCH_3), 3.85(s, 3H, OCH_3), 3.81(s, 3H, OCH_3), 2.35(s, 3H, CH_3). ^{13}C NMR (150 MHz, $CDCl_3$): 167.64, 161.01, 159.89, 159.55, 144.69, 140.61, 140.55, 131.80, 131.46, 129.95, 129.57(2), 128.06(2), 128.05(2), 123.53, 117.24, 114.39, 114.18(2), 101.81, 97.67, 57.73, 55.89, 55.43, 55.34, 21.47. MS (ESI) *m/z*: 445.12 $[M + H]^+$ (calcd for 445.19, $C_{28}H_{29}O_5$).

*4.1.2.3. 2,4-Dimethoxy-6-((E)-4-methoxystyryl)benzyl(E)-3-(2-methoxyphenyl)acrylate (**6c**).* White powder. Yield: 79.6%. m. p: 224–225 °C. ^{1}H NMR (500 MHz, $CDCl_3$): 8.01(d, J = 16.15 Hz, 1H, ArH), 7.45(m, 3H, ArH), 7.33(d, J = 15.85 Hz, 1H, ArH), 7.31(m, 1H, ArH), 6.98(d, J = 16.05 Hz, 1H, ArH), 6.89(m, 4H, ArH), 6.79(d, J = 2.25 Hz, 1H, ArH), 6.58(d, J = 16.10 Hz, 1H, ArH), 6.44(d, J = 2.25 Hz, 1H, ArH), 5.44(s, 2H, CH_2), 3.88(s, 3H, OCH_3), 3.85(s, 3H, OCH_3), 3.84(s, 3H, OCH_3), 2.81(s, 3H, OCH_3). ^{13}C NMR (150 MHz, $CDCl_3$): 167.86, 160.97, 159.91, 159.52, 158.38, 140.62, 140.23, 131.43, 131.32, 129.99, 129.14, 128.06(2), 123.57, 123.52, 120.63, 118.93, 114.50, 114.17(2), 111.06, 101.79, 97.68, 57.68, 55.89, 55.43, 55.41, 55.33. MS (ESI) *m/z*: 461.08 $[M + H]^+$ (calcd for 461.19, $C_{28}H_{29}O_6$).

*4.1.2.4. 2,4-Dimethoxy-6-((E)-4-methoxystyryl)benzyl(E)-3-(3-methoxyphenyl)acrylate (**6d**).* White powder. Yield: 68.4%. m.p: 208–210 °C. ^{1}H NMR (500 MHz, $CDCl_3$): 7.71(d, J = 16.00 Hz, 1H, ArH), 7.51(d, J = 8.70 Hz, 2H, ArH), 7.36(d, J = 16.05 Hz, 1H, ArH), 7.31(t, J = 7.85 Hz, 1H, ArH), 7.11(d, J = 6.12 Hz, 1H, ArH), 7.04(d, J = 16.10 Hz, 1H, ArH), 7.03(s, 1H, ArH), 6.95(m, 3H, ArH), 6.84(d, J = 2.20 Hz, 1H, ArH), 6.51(d, J = 15.35 Hz, 1H, ArH), 6.49(s, 1H, ArH), 5.50(s, 2H, CH_2), 3.93(s, 3H, OCH_3), 3.90(s, 3H, OCH_3), 3.86(s, 3H, OCH_3), 3.84(s, 3H, OCH_3). ^{13}C NMR (150 MHz, $CDCl_3$): 167.23, 161.05, 159.94, 159.83, 159.56, 144.62, 140.61, 131.51, 129.99, 129.82, 128.05(2), 123.47, 120.84, 118.62, 116.66, 116.25, 114.19(2), 113.14, 112.66, 101.82, 97.67, 57.85, 55.89, 55.44, 55.34, 55.27. MS (ESI) *m/z*: 461.08 $[M + H]^+$ (calcd for 461.19, $C_{28}H_{29}O_6$).

*4.1.2.5. 2,4-Dimethoxy-6-((E)-4-methoxystyryl)benzyl(E)-3-(4-methoxyphenyl)acrylate (**6e**).* White powder. Yield: 72.3%. m. p:

178–180 °C. ^{1}H NMR (500 MHz, $CDCl_3$): 7.65(d, J = 15.90 Hz, 1H, ArH), 7.46(d, J = 8.70 Hz, 2H, ArH), 7.41(d, J = 8.80 Hz, 2H, ArH), 7.32(d, J = 16.10 Hz, 1H, ArH), 6.98(d, J = 16.05 Hz, 1H, ArH), 6.87(m, 4H, ArH), 6.79(d, J = 2.15 Hz, 1H, ArH), 6.44(d, J = 2.25 Hz, 1H, ArH), 6.34(m, J = 15.90 Hz, 1H, ArH), 5.44(s, 2H, CH_2), 3.88(s, 3H, OCH_3), 3.85(s, 3H, OCH_3), 3.81(s, 6H, 2OCH_3). ^{13}C NMR (150 MHz, $CDCl_3$):167.61, 161.26, 160.99, 159.88, 159.54, 144.34, 140.59, 131.43, 129.96, 129.71(2), 128.05(2), 127.28, 123.55, 115.82, 114.45, 114.25(2), 114.17(2), 101.79, 97.67, 57.65, 55.89, 55.43, 55.36, 55.33. MS (ESI) *m/z*: 461.08 $[M + H]^+$ (calcd for 461.19, $C_{28}H_{29}O_6$).

4.1.2.6. 2,4-Dimethoxy-6-((E)-4-methoxystyryl)benzyl(E)-3-(benzo[d][1,3]dioxol-5-yl)acrylate ***(6f)***. White powder. Yield: 78.1%. m.p: 194–196 °C. ^{1}H NMR (500 MHz, $CDCl_3$): 7.58(d, J = 15.90 Hz, 1H, ArH), 7.45(d, J = 8.75 Hz, 2H, ArH), 7.30(d, J = 16.05 Hz, 1H, ArH), 6.98(d, J = 16.05 Hz, 1H, ArH), 6.95(m, 2H, ArH), 6.88(d, J = 8.75 Hz, 2H, ArH), 6.77(m, 2H, ArH), 6.43(d, J = 2.25 Hz, 1H, ArH), 6.28(d, J = 15.85 Hz, 1H, ArH), 5.97(s, 2H, CH_2), 5.42(s, 2H, CH_2), 3.88(s, 3H, OCH_3), 3.84(s, 3H, OCH_3), 3.81(s, 3H, OCH_3). ^{13}C NMR (150 MHz, $CDCl_3$): 167.43, 161.00, 159.87, 159.55, 149.47, 148.26, 144.36, 140.59. 131.44, 129.95, 128.97, 128.04(2), 124.36, 123.54, 116.30, 114.39, 114.18(2), 108.49, 106.52, 101.80, 101.50, 97.67, 57.70, 55.89, 55.43, 55.34. MS (ESI) *m/z*: 475.13 $[M + H]^+$ (calcd for 475.17, $C_{28}H_{27}O_7$).

4.1.2.7. 2,4-Dimethoxy-6-((E)-4-methoxystyryl)benzyl(E)-3-(2,3,4-trimethoxyphenyl)acrylate ***(6g)***. White powder. Yield: 66.4%. m.p: 201–203 °C. ^{1}H NMR (500 MHz, $CDCl_3$): 7.99(d, J = 16.10 Hz, 1H, ArH), 7.45(d, J = 8.70 Hz, 2H, ArH), 7.32(d, J = 16.05 Hz, 1H, ArH), 7.19(d, J = 8.80 Hz, 1H, ArH), 6.98(d, J = 16.00 Hz, 1H, ArH), 6.78(d, J = 2.30 Hz, 1H, ArH), 6.64(d, J = 8.85 Hz, 1H, ArH), 6.45(d, J = 16.10 Hz, 1H, ArH), 6.43(d, J = 2.30 Hz, 1H, ArH), 5.43(s, 2H, CH_2), 3.88(s, 3H, OCH_3), 3.86(s, 6H, 2OCH_3), 3.85(s, 3H, OCH_3), 3.84(s, 3H, OCH_3), 3.81(s, 3H, OCH_3). ^{13}C NMR (150 MHz, $CDCl_3$): 167.82, 160.96, 159.88, 159.22, 155.93, 155.39, 153.54, 141.95, 140.58, 139.66, 131.37, 129.99, 128.05(2), 123.57, 123.51, 117.24, 114.16(2), 107.62, 101.78, 97.68, 61.42, 60.90, 57.61, 56.04, 55.89, 55.43, 55.33. MS (ESI) *m/z*: 521.17 $[M + H]^+$ (calcd for 521.21, $C_{30}H_{33}O_8$).

4.1.2.8. 2,4-Dimethoxy-6-((E)-4-methoxystyryl)benzyl(E)-3-(3,4,5-trimethoxyphenyl)acrylate ***(6h)***. White powder. Yield: 72.7%. m. p: 191–193 °C. ^{1}H NMR (500 MHz, $CDCl_3$): 7.60(d, J = 15.90 Hz, 1H, ArH), 7.45(d, J = 8.70 Hz, 2H, ArH), 7.30(d, J = 16.05 Hz, 1H, ArH), 6.99(d, J = 16.00 Hz, 1H, ArH), 6.88(d, J = 8.70 Hz, 2H, ArH), 6.79(d, J = 2.25 Hz, 1H, ArH), 6.69(s, 2H, ArH), 6.44(d, J = 2.20 Hz, 1H, ArH), 6.38(d, J = 15.85 Hz, 1H, ArH), 5.44(s, 2H, CH_2), 3.88(s, 3H, OCH_3), 3.86(s, 3H, OCH_3), 3.85(s, 3H, OCH_3),3.83(s, 6H, 2OCH_3), 3.80(s, 3H, OCH_3). ^{13}C NMR (150 MHz, $CDCl_3$): 167.21, 161.06, 159.88, 159.57, 153.49, 153.36, 147.02, 144.61, 140.50, 139.91, 131.47, 129.52(2), 128.05, 123.41, 117.63, 114.18(2), 105.49(2), 105.10, 101.79, 97.68, 61.03, 57.80, 56.19, 56.10, 55.90, 55.44, 55.34. MS (ESI) *m/z*: 521.17 $[M + H]^+$ (calcd for 521.21, $C_{30}H_{33}O_8$).

4.1.2.9. 2,4-Dimethoxy-6-((E)-4-methoxystyryl)benzyl(E)-3-(4-fluorophenyl)acrylate ***(6i)***. White powder. Yield: 74.8%. m. p: 241–243 °C. ^{1}H NMR (500 MHz, $CDCl_3$): 7.64(d, J = 16.00 Hz, 1H, ArH), 7.44(m, 4H, ArH), 7.30(d, J = 16.05 Hz, 1H, ArH), 7.03(t, J = 8.10 Hz, 2H, ArH), 7.01(d, J = 16.05 Hz, 1H, ArH), 6.88(d, J = 8.70 Hz, 2H, ArH), 6.78(d, J = 2.20 Hz, 1H, ArH), 6.44(d, J = 2.20 Hz, 1H, ArH), 6.37(d, J = 15.95 Hz, 1H, ArH), 5.44(s, 2H, CH_2), 3.88(s, 3H, OCH_3), 3.85(s, 3H, OCH_3), 3.81(s, 3H, OCH_3). ^{13}C NMR (150 MHz, $CDCl_3$): 167.14, 165.03(d, J = 250.5 Hz), 161.05, 159.87, 159.57, 143.37, 140.59, 131.48, 130.33, 130.28(d, J = 60 Hz), 129.94, 128.04(2), 123.49, 116.27(d, J = 22.5 Hz), 114.18(2), 101.81, 97.67, 57.86, 55.89, 55.44, 55.34. MS (ESI) *m/z*: 449.14 $[M + H]^+$ (calcd for 449.17, $C_{27}H_{26}FO_5$).

4.1.2.10. 2,4-Dimethoxy-6-((E)-4-methoxystyryl)benzyl(E)-3-(3-chlorophenyl)acrylate ***(6j)***. White powder. Yield: 69.8%. m. p: 236–238 °C. ^{1}H NMR (500 MHz, $CDCl_3$): 7.59(d, J = 16.00 Hz, 1H, ArH), 7.45(d, J = 8.70 Hz, 2H, ArH), 7.41(s, 1H, ArH), 7.32–7.27(m, 3H, ArH), 7.29(d, J = 16.10 Hz, 1H, ArH), 6.98(d, J = 16.05 Hz, 1H, ArH), 6.89(d, J = 8.70 Hz, 2H, ArH), 6.78(d, J = 2.30 Hz, 1H, ArH), 6.45(d, J = 16.00 Hz, 1H, ArH), 6.43(d, J = 2.25 Hz, 1H, ArH), 5.44(s, 2H, CH_2), 3.88(s, 3H, OCH_3), 3.85(s, 3H, OCH_3), 3.81(s, 3H, OCH_3). ^{13}C NMR (150 MHz, $CDCl_3$): 166.80, 161.07, 159.86, 159.58, 143.03, 140.61, 136.34, 134.83, 131.51, 130.59, 130.06, 130.00, 129.89, 128.04(2), 127.87, 126.12, 123.48, 119.85, 114.19(2), 101.84, 97.66, 57.98, 55.89, 55.44, 55.34. MS (ESI) *m/z*: 465.61 $[M + H]^+$ (calcd for 465.14, $C_{27}H_{26}ClO_5$).

4.1.2.11. 2,4-Dimethoxy-6-((E)-4-methoxystyryl)benzyl(E)-3-(4-chlorophenyl)acrylate ***(6 k)***. White powder. Yield: 58.4%. m. p: 225–227 °C. ^{1}H NMR (500 MHz, $CDCl_3$): 7.62(d, J = 16.00 Hz, 1H, ArH), 7.45(d, J = 8.70 Hz, 2H, ArH), 7.37(d, J = 8.55 Hz, 2H, ArH), 7.31(m, 2H, ArH), 7.29(d, J = 15.95 Hz, 1H, ArH), 6.98(d, J = 16.05 Hz, 1H, ArH), 6.88(d, J = 8.70 Hz, 2H, ArH), 6.78(d, J = 2.25 Hz, 1H, ArH), 6.42(d, J = 16.15 Hz, 2H, ArH), 5.44(s, 2H, CH_2), 3.88(s, 3H, OCH_3), 3.85(s, 3H, OCH_3), 3.81(s, 3H, OCH_3). ^{13}C NMR (150 MHz, $CDCl_3$): 166.98, 161.06, 159.87, 159.58, 143.20, 140.59, 136.03, 133.01, 131.50, 129.90, 129.21(2), 129.11(2), 128.04(2), 123.47, 118.94, 114.18(2), 101.82, 97.47, 57.91, 55.89, 55.44, 55.34. MS (ESI) *m/z*: 465.61 $[M + H]^+$ (calcd for 465.14, $C_{27}H_{26}ClO_5$).

4.1.2.12. 2,4-Dimethoxy-6-((E)-4-methoxystyryl)benzyl(E)-3-(3-bromophenyl)acrylate ***(6l)***. White powder. Yield: 64.6%. m. p: 230–232 °C. ^{1}H NMR (500 MHz, $CDCl_3$): 7.59(d, J = 15.95 Hz, 1H, ArH), 7.58(s, 1H, ArH), 7.45(m, 3H, ArH), 7.36(d, J = 7.80 Hz, 1H, ArH), 7.29(d, J = 16.05 Hz, 1H, ArH), 7.21(t, J = 7.85 Hz, 1H, ArH), 6.99(d, J = 16.00 Hz, 1H, ArH), 6.89(d, J = 8.70 Hz, 2H, ArH), 6.78(d, J = 2.25 Hz, 1H, ArH), 6.45(d, J = 16.00 Hz, 1H, ArH), 6.43(d, J = 2.25 Hz, 1H, ArH), 5.45(s, 2H, CH_2), 3.88(s, 3H, OCH_3), 3.85(s, 3H, OCH_3), 3.81(s, 3H, OCH_3). ^{13}C NMR (150 MHz, $CDCl_3$): 166.76, 161.07, 159.86, 159.58, 142.92, 140.60, 136.62, 132.91, 131.51, 130.82, 129.90, 128.04(2), 126.91, 126.55, 123.48, 122.94, 119.87, 114.20(2), 114.16, 101.84, 97.65, 57.98, 55.88, 55.44, 55.35. MS (ESI) *m/z*: 509.16 $[M + H]^+$ (calcd for 509.09, $C_{27}H_{26}BrO_5$).

4.1.2.13. 2,4-Dimethoxy-6-((E)-4-methoxystyryl)benzyl(E)-3-(4-bromophenyl)acrylate ***(6m)***. White powder. Yield: 68.3%. m.p: 244–246 °C. ^{1}H NMR (500 MHz, $CDCl_3$): 7.60(d, J = 16.00 Hz, 1H, ArH), 7.46(m, 4H, ArH), 7.30(d, J = 8.50 Hz, 2H, ArH), 7.29(d, J = 16.15 Hz, 1H, ArH), 6.97(d, J = 16.05 Hz, 1H, ArH), 6.88(d, J = 8.70 Hz, 2H, ArH), 6.78(d, J = 2.25 Hz, 1H, ArH), 6.43(d, J = 2.25 Hz, 1H, ArH), 6.42(d, J = 16.00 Hz, 1H, ArH), 5.44(s, 2H, CH_2), 3.88(s, 3H, OCH_3), 3.85(s, 3H, OCH_3), 3.82(s, 3H, OCH_3). ^{13}C NMR (150 MHz, $CDCl_3$): 166.96, 161.06, 159.86, 159.58, 143.27, 140.59, 133.44(2), 132.07, 131.50, 129.90(2), 129.43(2), 128.04, 124.38, 123.47, 119.06, 114.18(2), 101.18, 101.82, 97.66, 57.93, 55.89, 55.44, 55.35. MS (ESI) *m/z*: 509.16 $[M + H]^+$ (calcd for 509.09, $C_{27}H_{26}BrO_5$).

4.1.2.14. 2,4-Dimethoxy-6-((E)-4-methoxystyryl)benzyl(E)-3-(4-nitrophenyl)acrylate ***(6n)***. Yellow powder. Yield: 54.4%. m.p: 256–258 °C. ^{1}H NMR (500 MHz, $CDCl_3$): 8.20(d, J = 8.75 Hz, 2H, ArH), 7.68(d, J = 16.00 Hz, 1H, ArH), 7.58(d, J = 8.75 Hz, 2H, ArH), 7.45(d, J = 8.70 Hz, 2H, ArH), 7.28(d, J = 16.05 Hz, 1H, ArH), 6.99(d, J = 16.05 Hz, 1H, ArH), 6.89(d, J = 8.70 Hz, 2H, ArH), 6.78(d, J = 2.25 Hz, 1H, ArH), 6.56(d, J = 16.05 Hz, 1H, ArH), 6.44(d,

J = 2.25 Hz, 1H, ArH), 5.47(s, 2H, CH_2), 3.89(s, 3H, OCH_3), 3.85(s, 3H, OCH_3), 3.81(s, 3H, OCH_3). ^{13}C NMR (150 MHz, $CDCl_3$): 166.24, 161.17, 159.86, 159.62, 148.40, 141.66, 140.65, 140.60, 131.58, 129.85, 128.59(2), 128.04(2), 124.12(2), 123.38, 122.69, 114.20(2), 113.91, 101.85, 97.66, 58.26, 55.59, 55.45, 55.35. MS (ESI) *m/z*: 476.28 $[M + H]^+$ (calcd for 476.16, $C_{27}H_{26}NO_7$).

*4.1.2.15. 2,4-Dimethoxy-6-((E)-4-methoxystyryl)benzyl(E)-3-(4-(trifluoromethyl)phenyl)acrylate (**6o**)*. Yellow powder. Yield: 57.6%. m. p: 249–251 °C. ^1H NMR (500 MHz, $CDCl_3$): 7.67(d, J = 16.00 Hz, 1H, ArH), 7.60(d, J = 8.30 Hz, 2H, ArH), 7.54(d, J = 8.25 Hz, 2H, ArH), 7.45(d, J = 8.70 Hz, 2H, ArH), 7.29(d, J = 16.05 Hz, 1H, ArH), 6.99(d, J = 16.00 Hz, 1H, ArH), 6.88(d, J = 8.75 Hz, 2H, ArH), 6.78(d, J = 2.25 Hz, 1H, ArH), 6.51(d, J = 16.05 Hz, 1H, ArH), 6.44(d, J = 2.30 Hz, 1H, ArH), 5.46(s, 2H, CH_2), 3.89(s, 3H, OCH_3), 3.85(s, 3H, OCH_3), 3.81(s, 3H, OCH_3). ^{13}C NMR (150 MHz, $CDCl_3$): 166.65, 161.11, 159.87, 159.59, 142.77, 140.61, 137.88, 131.55, 129.88, 128.15(2), 128.05(2), 125.81, 125.78, 123.43, 120.93, 114.19(2), 114.06(2), 101.84, 97.66, 58.09, 55.89, 55.44, 55.34. MS (ESI) *m/z*: 499.21 $[M + H]^+$ (calcd for 499.17, $C_{28}H_{26}F_3O_5$).

4.2. Pharmacology

4.2.1. Antiproliferative assay

Human liver carcinoma cell line HepG2, human non-small-cell-lung cancer cell line A549, human epithelial cervical cancer cell line HeLa, human breast cancer cell line MCF-7 and MDA-MB-231, human embryonic kidney cell 293T and human liver cell (LO2) were employed to evaluate the antiproliferative activity using MTT assay. Briefly, cells in logarithmic phase were harvested and divided into 96-well plates (0.5×10^4 each well), culture medium containing the test compounds at different concentrations was added to each well. After incubating for 48 h, MTT (5 mg/mL in PBS) was added and incubated for more 4 h. Discarding the suspension and 150 μL DMSO was added and shaking for 10 min, plates were read in Infinite® M200 Pro Multimode Microplate Reader (Tecan, Switzerland) at the wavelength of 570 nm (reference wavelength 650 nm). Triplicate wells were used for each concentration and each assay was carried out at least three times. The cytotoxic activity was expressed as the IC_{50} values.

4.2.2. Tubulin polymerization inhibitory assay

A solution of tubulin (3 mg/mL) in was prepared G-PEM buffer which was composed of 80 mM PIPES pH 6.9, 2 mM $MgCl_2$, 0.5 mM EGTA, 9.2% glycerol and 0.9 mM GTP, and then the test compounds were added. The mixture was preincubated in ice-bath. After 30 min, the absorbance was detected by a spectrophotometer at 340 nm at 37 °C every 2 min over 60 min.

4.2.3. Competitive inhibition assays

Radiolabeled [^{3}H] colchicine competition scintillation proximity (SPA) assay was employed to evaluate for competitive binding activity of tested compounds. Briefly, the reaction mixtures contained 4 μM [^{3}H] colchicine, tested compounds with different concentration, a 100 μL buffer including modified tubulin (1 μM), 80 mM PIPES (pH 6.8), 1 mM EGTA, 10% glycerol, 1 mM $MgCl_2$, and 1 mM GTP, and were incubated for 2 h at 37 °C. The radioactive counts were measured using scintillation counter.

4.2.4. Cell cycle assay

MCF-7 cells in exponential growth was seeded into 6-well plate and every well contained approximately 1×10^5, they were incubated for 12 h, and then treated with compound **6h** at different concentrations for 24 h. The cells were collected and fixed with 70% ethanol at 4 °C for 12 h. The fixed cells were incubated with 100 ml RNase A and stained with PI for 30 min. The DNA content of the cells was gathered on FACS Calibur flow cytometer (Bectone Dickinson, San Jose, CA, USA).

4.2.5. Cell apoptosis assay

1×10^5 MCF-7 cells in exponential growth was seeded into each well of 6-well plate, and treated with compound **6h** at different concentrations for 24 h, the cells were collected, centrifuged and re-suspended in 500 ml AnnexinV binding buffer, and incubated for 15 min on the ice in the darkness. Samples were analyzed using a FACS Calibur flow cytometer (Bectone Dickinson, San Jose, CA, USA).

4.2.6. Western blotting

MCF-7 cells were incubated in the presence of **6h** for 24 h. Subsequently, trypsinized the cells and collected, the prepared 1 × RIPA lysis buffer (1% NP-40,50 mM Tris-HCl, 150 mM NaCl, pH 7.4, 0.25% deoxycholic acid, 1 mM EDTA containing protease inhibitors PMSF) (Amresco, Solon, USA) was added to extract the total proteins. The proteins was separated by sodium dodecyl sulfate (8% or 10%) polyacrylamide gel electrophoresis (SDS-PAGE, BioRad Laboratories, Hercules, CA), and transferred from the gel onto to PVDF membrane (BioRad Laboratories, Hercules, CA), blotted with primary antibodies, probed with secondary isotype specific antibodies tagged with horseradish peroxidase (Cell Signaling Technology). Bound immunocomplexes were detected using a ChemiDOC™ XRS + system (BioRad Laboratories, Hercules, CA).

4.2.7. Immunofluorescence staining

MCF-7 cells were seeded into 6-well plates and then treated with different concentrations of tested compounds. Cells on cover slips were fixed by 4% paraformaldehyde. After permeabilized with 1% Triton X-100, cells were incubated in 3% BSA for 1 h. Then cells were incubated with anti b-tubulin monoclonal antibody at 500-fold dilution overnight at 4 °C and stained with Cy3-labeled rabbit anti-mouse secondary antibody at 500-fold dilution. Then DNA of cells were detected with DAPI. Cells were finally visualized using an LSM 570 laser confocal microscope (Carl Zeiss, Germany).

4.2.8. Molecular docking

Docking study was performed by Discovery Studio 3.5 and the tubulin protein (PDB:1SA0) was downloaded from RCSB Protein Date Bank (www.rcsb.org). The protein and all ligands were prepared by minimization with CHARMM force field. Molecular docking was carried out using DS-CDOCKER protocol without constraint, all bound water and ligands were eliminated from the protein and the polar hydrogen was added to the proteins.

Acknowledgments

This work was supported by National Natural Science Foundation of China (81602985 and 81703754), the Fundamental Research Funds for the Central Universities (2632018ZD19 and 2632018ZD18), the Natural Science Foundation of Jiangsu Province (BK20160763), the Program for Chang jiang Scholars and Innovative Research Team in University (IRT_15R63), the 111 Project from Ministry of Education of China and the State Administration of Foreign Export Affairs of China (B18056) and the "Double First-Class" University Project (CPU2018GF03).

Appendix A. Supplementary material

Supplementary data to this article can be found online at https://doi.org/10.1016/j.bioorg.2019.103319.

References

[1] K. Harindranath, R.V. Hofele, B. Jacek, K. Satish, T. Katharina, U. Henning, M. Eckhard, Z. Markus, Tau stabilizes microtubules by binding at the interface between tubulin heterodimers, P. Natl. Acad. Sci. U.S.A. 112 (2015) 7501–7506.
[2] A. Anna, M.O. Steinmetz, Control of microtubule organization and dynamics: two

ends in the limelight, Nat. Rev. Mol. Cell. Bio. 16 (2015) 711–726.
[3] A. Muroyama, T. Lechler, Microtubule organization, dynamics and functions in differentiated cells, Development 144 (2017) 3012–3021.
[4] D. Charles, J. Mary Ann, Microtubule-binding agents: a dynamic field of cancer therapeutics, Nat. Rev. Drug. Discov. 9 (2010) 790–803.
[5] J. Mary Ann, W. Leslie, Microtubules as a target for anticancer drugs, Nat. Rev. Cancer 4 (2004) 253–265.
[6] M.A. Jordan, K. Kamath, How do microtubule-targeted drugs work? An overview, Curr. Cancer Drug Targets 7 (2007) 730–742.
[7] P. Federico, D.R. Budman, Review: tubulin function, action of antitubulin drugs, and new drug development, Cancer Invest. 23 (2005) 264–273.
[8] M. Ingrid, P. Ludovic, D. Audrey, K. Manikandan, R.B.G. Ravelli, D. Birgit, P. Andreas, K. Marcel, G. Beno T, Design and characterization of modular scaffolds for tubulin assembly, J. Biol. Chem. 287 (2012) 31085–31094.
[9] M.A. Jordan, K. Wendell, S. Gardiner, W.B. Derry, H. Copp, L. Wilson, Mitotic block induced in HeLa cells by low concentrations of paclitaxel (Taxol) results in abnormal mitotic exit and apoptotic cell death, Cancer Res. 56 (1996) 816–825.
[10] R. Kaur, G. Kaur, R.K. Gill, R. Soni, J. Bariwal, Recent developments in tubulin polymerization inhibitors: An overview, Eur. J. Med. Chem. 87 (2014) 89–124.
[11] E. Mukhtar, V.M. Adhami, H. Mukhtar, Targeting microtubules by natural agents for cancer therapy, Mol. Canc. Therapeut. 13 (2014) 275–284.
[12] V. Ilio, G. Lorenzo, C. Maria, K. Guido, Mitotic catastrophe: a mechanism for avoiding genomic instability, Nat. Rev. Mol. Cell. Bio. 12 (2011) 385–392.
[13] J. Xi, X. Zhu, Y. Feng, N. Huang, G. Luo, Y. Mao, X. Han, W. Tian, G. Wang, X. Han, Development of a novel class of tubulin inhibitors with promising anticancer activities, Mol. Cancer Res. Mcr 11 (2013) 856–864.
[14] R.B.G. Ravelli, G. Beno T, P.A. Curmi, J. Isabelle, L. Sylvie, S. André, K. Marcel, Insight into tubulin regulation from a complex with colchicine and a stathmin-like domain, Nature 428 (2004) 198–202.
[15] B. Bhabatarak, P. Dulal, G. Suvroma, B. Mithu, Anti-mitotic activity of colchicine and the structural basis for its interaction with tubulin, Med. Res. Rev. 28 (2010) 155–183.
[16] L. Ling, S. Jiang, X. Li, L. Yao, S. Jing, J. Chen, Recent advances in trimethoxyphenyl (TMP) based tubulin inhibitors targeting the colchicine binding site, Eur. J. Med. Chem. 151 (2018) 482–494.
[17] L. Peng, Q. Yan, W. Lingying, Y. Sheng, L. Nan, W. Haijun, X. Haiyan, S. Kelin, Z. Shuxiang, H. Xiaohong, A phase I clinical trial assessing the safety and tolerability of combretastatin A4 phosphate injections, Anti-Cancer Drug 25 (2014) 462–471.
[18] Y. Lu, J. Chen, M. Xiao, W. Li, D.D. Miller, An overview of tubulin inhibitors that interact with the colchicine binding site, Pharm. Res. 29 (2012) 2943–2971.
[19] S.K. Tahir, E.K. Han, B. Credo, H.S. Jae, J.A. Pietenpol, C.D. Scatena, J.R. Wu-Wong, D. Frost, H. Sham, S.H. Rosenberg, A-204197, a new tubulin-binding agent with antimitotic activity in tumor cell lines resistant to known microtubule inhibitors, Cancer Res. 61 (2001) 5480–5485.
[20] K. Chen, Y.L. Zhang, J. Fan, X. Ma, H.L. Zhu, Novel nicotinoyl pyrazoline derivates bearing N-methyl indole moiety as antitumor agents: Design, synthesis and evaluation, Eur. J. Med. Chem. 156 (2018) 722–737.
[21] Y. Zhang, B. Li, R. Yang, L. Xia, A. Fan, Y. Chu, L. Wang, Z. Wang, A. Jiang, H. Zhu, A class of novel tubulin polymerization inhibitors exert effective anti-tumor activity via mitotic catastrophe, Eur. J. Med. Chem. 163 (2018) 896–910.
[22] H. Mirzaei, S. Emami, Recent advances of cytotoxic chalconoids targeting tubulin polymerization: Synthesis and biological activity, Eur. J. Med. Chem. 121 (2016) 610–639.
[23] M. Jang, L. Cai, G.O. Udeani, K.V. Slowing, C.F. Thomas, C.W. Beecher, H.H. Fong, N.R. Farnsworth, A.D. Kinghorn, R.G. Mehta, Cancer chemopreventive activity of resveratrol, a natural product derived from grapes, Science 275 (1997) 218–220.
[24] P. Signorelli, R. Ghidoni, Resveratrol as an anticancer nutrient: molecular basis, open questions and promises, J. Nutr. Biochem. 16 (2005) 449–466.
[25] M.J. Pérez-Pérez, E.M. Priego, O. Bueno, M.S. Martins, M.D. Canela, S. Liekens, Blocking blood flow to solid tumors by destabilizing tubulin: an approach to targeting tumor growth, J. Med. Chem. 59 (2016) 8685–8711.
[26] J. Pan, T. Xu, F. Xu, Y. Zhang, Z. Liu, W. Chen, W. Fu, Y. Dai, Y. Zhao, J. Feng, Development of resveratrol-curcumin hybrids as potential therapeutic agents for inflammatory lung diseases, Eur. J. Med. Chem. 125 (2017) 478–491.
[27] X.F. Huang, B.F. Ruan, X.T. Wang, C. Xu, H.M. Ge, H.L. Zhu, R.X. Tan, Synthesis and cytotoxic evaluation of a series of resveratrol derivatives modified in C2 position, Eur. J. Med. Chem. 42 (2007) 263–267.